International Journal of Applied Engineering Research
ISSN 0973-4562 Volume 10, Number 6 (2015) pp. 13789-13802

http://www.ripublication.com

Automatic Renal Neoplasm Volumetry on Prior Shape Level Set Segmentation Method

Prof. K.Sudhakar[#1], Prof. D.Satheesh Kumar[#2], Prof.B.Rajesh Kumar[#3]
[#]Department of Computer Science and Engineering,
Hindusthan College of Engineering and Technology,
Coimbatore, Tamil Nadu, India- 641 032.
[3]AP/CSE, RVS College of Engineering and Technology, Coimbatore, India.
[1]sudhak.be@gmail.com [2]dsatheeshme@gmail.com

Abstract

Fully automatic 3-D segmentation techniques for clinical applications or epidemiological studies have proved to be a very challenging task in the domain of medical image analysis. The 3-D organ segmentation on Magnetic Resonance (MR) datasets needs a well-designed segmentation strategy due to partial volume effects, imaging artifacts, and similar tissue properties of adjacent tissues. A 3-D segmentation framework for totally automatic excretory organ parenchyma volumetry that uses Bayesian concepts for probability map generation was developed. The likelihood map quality is improved in a very multistep refinement approach. An extended previous form level set segmentation method is then applied on the refined probability maps. We improved the quality of segmentation by incorporating an exterior cortex edge alignment technique using cortex probability maps. In contrast to previous approaches, we tend to combine several relevant kidney parenchyma features in a sequence of segmentation techniques for successful parenchyma delineation on native MR Datasets. The proposed method is also able to acknowledge and exclude parenchymal cysts from the parenchymal volume. We have analyzed four different quality measures showing higher results for right parenchymal tissue than for left parenchymal tissue due to an incorporated liver part removal in the segmentation framework. Our result shows that, the outer cortex edge alignment approach successfully improves the quality measures.

Keywords: Bayesian probability, distance transform, Fourier descriptors, prior shape, three-dimensional (3-D) level set segmentation.

Introduction

The demand of medical image segmentation for clinical applications and (bio) medical research topics increased substantially. A renal neoplasm could be a assortment of abnormal cells or tissues originating inside the kidney. The formation of a renal neoplasm may contribute to the development of a benign cyst or malignant neoplasm. Extensive testing is important for determining the composition of a neoplastic growth. When the renal neoplasm is determined to be malignant neoplasm, then a diagnosis of kidney cancer is confirmed. The malignant renal neoplasm treatment depends on many factors, including the staging and type of neoplasm and also the individual's overall health. It is unknown what initiates and promotes the abnormal cell development related to the formation of a renal neoplasm. The previous research demonstrated that the process could begin with a mutation that happens throughout cell development that causes fast cellular division and maturation. As the cells divide and grow, they will accumulate together to form neoplasm, or tumor. As a time constraint, some cells could break off from the cluster to jaunt alternative parts of the body spreading their virulence and metastasize. Individuals with a renal neoplasm may not experience any symptoms during the early stages of neoplastic growth. When the tumour matures, individuals may begin to exhibit a variety of signs that may include weight loss, lower back pain, and bloody urine. Additional generalized symptoms may include fatigue and fever. In community medicine, medical image segmentation enables quantification of certain health-related properties in populations accelerating research insights in the domain of modern epidemiological science. Organ volumetry is of special interest requiring organ segmentation in 3-D medical datasets. Manual segmentation of 3-D datasets is inappropriate for epidemiological studies because of the large amounts of data. Hence, this time-consuming task cannot be accomplished efficiently by radiologists. The work presented here is designed for a population-based study [Study of Health In Pomerania (SHIP)] in which automatic kidney parenchyma volumetry for Magnetic Resonance Images (MRI) is required. Our fully automatic method can be directly applied for epidemiological studies. The situation in an epidemiological study differs from a clinical analysis scenario. Data from several thousand subjects are acquired over a long period of time which is to be analyzed during and potentially long after the acquisition process has ended. This has consequences for the analysis process. First of all, the method should not require interaction for single cases. Second, the method should depend as little as possible on the accuracy of domain knowledge. Based on a representative test dataset the degree as to which domain knowledge is integrated into the analysis is usually determined. With ongoing image acquisition, the view on what is representative may change, however.

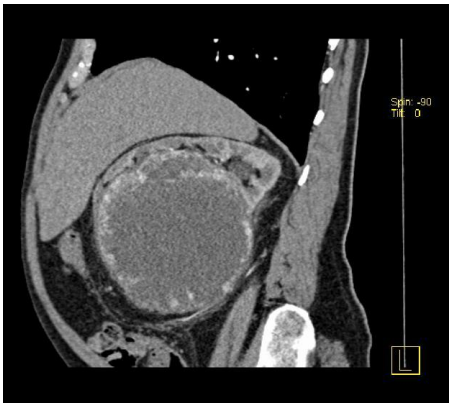

Figure 1.1: Human Kidney Diagram

Finally, the method should be based on the specific analysis questions but it should be sufficiently modularized to enable variations of such questions. In contrast to earlier approaches we use all important kidney features in MRI datasets for segmentation. For keeping the method as modular as possible and for making the method robust with respect to small changes of necessary domain knowledge, we selected a sequence of processes to arrive at the result. At each step, the accuracy of the result is improved by adding new knowledge about the appearance of the kidney to the result from the previous step. First, probability maps are generated and refined from known kidney features. Subsequent level set segmentation segments the kidney parenchyma in these maps by incorporating the trained 3-D shapes of kidney parenchymas. The level set method is steered by three forces. It uses those probability maps as data-driven force, prior knowledge of trained 3-D distance maps of kidney parenchymas as shape-driven force, and extracted information about outer cortex edges as alignment force. In our case, the goal was volumetry of the renal parenchyma in a general population. Cases of renal cancer were excluded from automatic renal parenchyma volumetry and are not considered in our framework. Parenchymal cyst volume has to be accounted for but their volume has to be excluded for epidemiological research, since it does not contribute to renal functions like nonpathological parenchymal tissue. Our framework is able to exclude renal cystic volume from the parenchymal volume. Surgery is the initial approach used to treat kidney cancer. The procedure is also conducted one among two ways in which depending on the extent of the malignancy and condition of the kidney. The affected region may be either partially or fully removed. A nephron-sparing surgery could also be conducted laparoscopically or as an open procedure, requiring one massive incision, and involves the removal of the tumor and a small portion of the surrounding, healthy tissue. The procedure is known as a nephrectomy, when the whole kidney is removed. It necessitates not only the removal of the kidney, but also the moderate portion of surrounding healthy tissue and nearby lymph nodes.

Once surgery is not possible due to the health of the individual, non-surgical choices could also be utilized that involve the employment of embolization, radiofrequency ablation, or cryoablation. The procedure wherever the tumor's blood

supply is cut off with the help of a unique material injected into the main blood vessel is called Embolization. When conducted with the aid of imaging technology, the radiofrequency ablation uses the application of an electrical current via a needle to focus on and eradicate cancerous cells with the help of heat. Cryoablation also utilizes imaging technology and involves the freezing of cancerous cells through the utilization of a gas-delivering needle.

Related Works

A probabilistic deformable model for the representation of multiple brain structures has been explained. The statistically learned deformable model represents the relative location of different anatomical surfaces in brain Magnetic Resonance Images (MRIs) and accommodates their significant variability across different individuals [1]. The surfaces of each anatomical structure are parameterized by the amplitudes of the vibration modes of a deformable spherical mesh [1]. In the training set, for a given MRI a vector containing the largest vibration modes describing the different deformable surfaces is created. In M. Prastawa et al.[2], the detection of edema is done with tumor segmentation, which is important for diagnosis, planning, and treatment. They proposed a method which does not require contrast enhanced image channels but many other tumor segmentation methods rely on the intensity enhancement produced by the gadolinium contrast agent in the T1-weighted image. The T2 MR image channel is the only required input for the segmentation procedure, but it additionally uses non-enhanced image channels for improved tissue segmentation. It is noted that, acquisition of non-contrast agent cine Cardiac Magnetic Resonance (CMR) gated images through the cardiac cycle is a well-established part of examining cardiac global function [3]. They proposed an automated framework for analyzing the wall thickness and thickening function on these images that consists of three main steps. With a geometric deformable model guided by a special stochastic speed relationship, first, inner and outer wall borders are segmented from their surrounding tissues. Level set evolution combining global smoothness with the flexibility of topology changes offers significant advantages over the conventional statistical classification. Level set evolution with constant propagation needs to be initialized either completely inside or outside the tumor and can leak through weak or missing boundary parts. By statistical force, constant propagation term was replaced to overcome these limitations which results in a convergence to a stable solution.

Methodology

Existing Method

Manual segmentation of 3-D datasets is inappropriate for epidemiological studies because of the large amounts of data. Hence, this time-consuming task cannot be accomplished efficiently by radiologists in hospitals Automatic segmentation would be much more appropriate; however, it is a difficult task due to the complexity in medical image understanding requiring trained skills of medical experts. Although

many contributions to organ segmentation (i.e., segmentation of liver, brain, lung, and kidney) can be found in the literature, it is still challenging because of the complexity of the information in the data. Hence, most proposed methods require some kind of human interaction during segmentation. For epidemiological studies, this is a serious drawback.

Disadvantages
Data from several thousand subjects are acquired over a long period of time which is to be analyzed during and potentially long after the acquisition process has ended. This has consequences for the analysis process. First of all, the method should not require interaction for single cases. Secondly, the method should depend as little as possible on the accuracy of domain knowledge. The degree as to which domain knowledge is integrated into the analysis is usually determined based on a representative test dataset. With ongoing image acquisition, the view on what is representative may change, however. Thirdly, the method should be based on the specific analysis questions but it should be sufficiently modularized to enable variations of such questions. In contrast to earlier approaches we use all important kidney features in MRI datasets for segmentation.

Proposed Method
In our proposed method, we selected a sequence of processes to arrive at the result. At each step, the accuracy of the result is improved by adding new knowledge about the appearance of the kidney to the result from the previous step. First, probability maps are generated and refined from known kidney features. Subsequent level set segmentation segments the kidney parenchyma in these maps by incorporating the trained 3-D shapes of kidney parenchymas. The level set method is steered by three forces. It uses those probability maps as data-driven force, prior knowledge of trained 3-D distance maps of kidney parenchymas as shape-driven force, and extracted information about outer cortex edges as alignment force.

Advantages
In our case, the goal was volumetry of the renal parenchyma in a general population. Cases of renal cancer were excluded from automatic renal parenchyma volumetry and are not considered in our framework. Parenchymal cyst volume has to be accounted for but their volume has to be excluded for epidemiological research, since it does not contribute to renal functions like nonpathological parenchymal tissue. Our framework is able to exclude renal cystic volume from the parenchymal volume.

Our Contribution

Given Methods discussed so far incorporate only few kidney features (i.e., mainly intensities or 3-D shape), which is not sufficient for parenchyma volumetry on native MR Datasets. The performance of a method depends on the accuracy of domain knowledge and the extent of redundancy between domain knowledge and data information. However, this could mean that—considering the potential life span of

SHIP of more than 20 years—older results need constantly be recomputed with new data being acquired. We are interested in using qualitative domain knowledge since it is less likely those qualities (such as the horseshoe-like shape of the kidney in some slices) need to be changed. For using them in a computer algorithm, qualities need to be quantified nonetheless but we strive for types of domain knowledge that is characterized by few parameters and where the dependency of the results on the exact parameterization is low. If needed, these parameters could and will be adapted, of course. Since this will make new results incomparable to earlier results, a list of parameter settings will be part of any analysis using our system.

For being less dependent on specific apriori knowledge, we use all possible kinds of domain knowledge at different stages of processing. We perform the segmentation methods in automatically predefined regions for left and right kidneys to avoid time-consuming searching in the complete MR Dataset. By using prior information about cortex extensions, we are able to remove liver parts enhanced in cortex probability maps that assist in delineation of right kidney parenchyma. We recognize connectivity properties between parenchyma and adjacent tissue and incorporate this information into Bayesian probability maps of parenchyma intensities. During this process we use knowledge about characteristic 2-D horseshoe forms of inner transversal kidney slices to recognize and separate parenchyma labels from surrounding tissue. Opposed to existing approaches, we do not apply segmentation techniques on original data but perform our optimization strategies for segmentation directly in probability maps, which enhance already selected parenchyma features. In the last segmentation step we apply 3-D prior shape knowledge of renal parenchyma in an extended level set segmentation approach and support the propagation process by outer cortex edge alignment showing improved results for the underlying prior shape level set approach. This makes recognition and delineation of renal parenchyma robust to inaccuracies in the domain knowledge. Furthermore, we extend our approach to a fully automatic parenchyma volumetry framework to be a helpful and efficient assistance in population-based studies and large patient populations. Our approach is also able to recognize and exclude renal cystic volumes from renal parenchymal volumes.

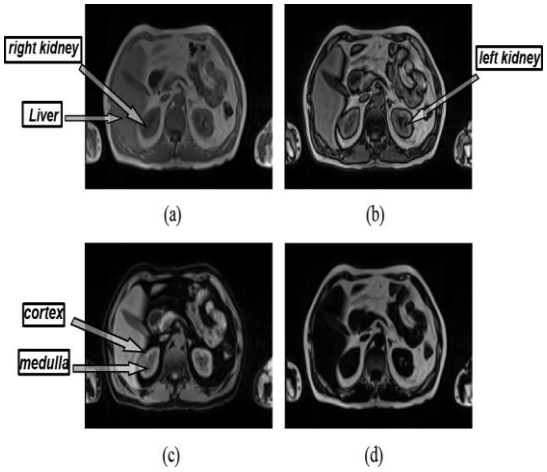

Figure 4.1: Original MR Images

Our proposed work is a multistep approach that gradually accumulates information until the final result is produced. We will present relevant steps independently, justify their usage, and describe their combined effects. The modularization of the proposed framework is subdivided into a training and application phase.

A. Denoising of MR Datasets

We tested several linear and nonlinear filter methods to denoise the original MR Datasets. Gaussian and median filters blurred relevant edges between adjacent but different tissues. Hence, standard anisotropic diffusion by Perona and Malik [21] was compared with a modified curvature diffusion equation of Whitaker and Xue [22]. Since the results from applying the method of [22] show more homogenized intensities for the different tissue types and preserve relevant edge magnitudes, we decided to apply this Denoising method. For further segmentation we used the denoised MR Datasets of the fat-saturated weighting which shows the most distinctive information between medulla and cortex.

B. Determination of Most Likely Kidney Regions

During image acquisition, all probands are placed inside the tomography in a similar way. Kidney locations—despite of different proband's height and weight—are to be expected at similar locations in the MR-dataset. We merge all the trained renal parenchyma masks to generate two binary masks representing ROIs for left and right kidney parenchyma, respectively. These ROIs are the most likely kidney regions. As long as the MLKR completely encloses the kidney, the speed of the following steps is influenced only by estimation errors. We undergo a morphological dilation with a spherical structuring element.

C. Probability Map Generation

To generate probability maps we divided the MR intensities inside the MLKR into the two classes, **rpc** (renal parenchyma) and **bg_rpc** (background) from voxels in the vicinity of the renal parenchyma mask. The background intensity histogram is generated by the samples of the trained background masks of the training phase. Samples of the trained parenchyma masks and remaining adjacent tissue generate the histogram Likelihood functions for the two classes and estimated convolving the intensity histograms with a Gaussian kernel (standard deviation 2.5). Parzen windowing with a Gaussian, smoothes the histogram without enforcing a particular type of distribution function. The Bayesian theorem then states that,

$$P_{rpc} = \frac{p(I|rpc).pr(rpc)}{p(I|rpc).pr(rpc) + p(I|bg_{rpc}).pr(bg_{rpc})}$$

D. Liver Part Removal

Liver and renal cortex show similar intensities in the MR Datasets of the study (see Fig.4. 1). Since the liver is the biggest abdominal organ, the maximal cortex thickness can be assumed to be lower than the spatial extent of the liver. We adopt the empirically determined maximum cortex thickness from the training phase mm to

remove liver parts from the maps. We begin with liver part removal by maximum a posteriori classification between the liver and cortex tissue (summarized in the class) and the background of a posteriori probability maps for the two classes calculated by the Bayesian formulations based on (2) to generate a binary livercortex mask .We generate a signed distance function representing distances to the boundary of the liver-cortex mask according to

$$d_{ctx}\left((x_f\, y_f\, , z_f)\middle| M_{ctx}(x_f\, y_f\, , z_f) = 1\right) = \min_{\{(x_b,y_b,z_b)|M_{ctx}(x_b,y_b,z_b)=0\}} (\left\| (x_f\, y_f\, , z_f)^T - (x_b y_b, z_b)^T \right\|)$$

and

$$d_{ctx}\left((x_b y_b, z_b)\middle| M_{ctx}(x_b y_b, z_b) = 0\right) = -\min_{\{(x_f\, y_f\, ,z_f)|M_{ctx}(x_f\, y_f\, ,z_f)=1\}} (\left\| (x_f\, y_f\, , z_f)^T - (x_b y_b, z_b)^T \right\|)$$

E. Probability Map Refinement Using 2-D Shape Differences

Even after liver removal the intensity distribution is not unique for the renal parenchyma, and map (volume) calculated by maximum a posteriori classification of the renal parenchyma based on a posteriori probability determinations often contains erroneous segmentations. Hence, by an additional morphological operation, we determine subparts that may not be part of the parenchyma and reduce the probability in these subparts. However, due to different shape, organ size and abdominal fat quota of the participants, the manner of surface contacts between their abdominal organs differs strongly. Nonetheless, transition regions between the kidney and adjacent organs or tissue types are characterized by small bridge-like structures. The purpose of the morphological operation is to break up the current estimate of the volume at those locations. Shape information is then used to determine which of the part volumes most likely the renal parenchyma is. Fourier descriptors are now computed for each 2-D connected component in all slices of all subvolumes. Since the maximum a posteriori renal parenchyma shapes can include the renal pelvis, 2-D morphological erosion process with a small disk-like structuring element for every 2-D connected component before we determine their Fourier descriptors is done. Dissimilarity D is then computed as the squared norm of the difference between the Fourier descriptors

$$D_{mean}(F_{jk}) = \frac{1}{M} \cdot \sum_{i=1}^{M} D(F_{i,}\, F_{jk})$$

F. Prior Shape Level Set Segmentation

The corrected parenchyma probability map attenuates tissue regions whose renal parenchyma assignment has low probability. The resulting volume of the probability map refinement methods improves the initial maximum posteriori segmentation result significantly, but may still contain erroneous segmentations. Furthermore, we cannot

guarantee that all non-parenchyma tissue is significantly suppressed on the probability maps. However, we can use as suitable underlying dataset for the 3-D level set segmentation. In the following, the prior shape level set segmentation combines the data information with prior shape information of 3-D parenchyma shapes contained in the parenchyma masks of the training phase. The incorporation of prior shape information uses knowledge about the expected 3-D parenchyma shape, which is an important feature for parenchyma recognition, accelerates the segmentation process and reduces the amount of local minima that do not represent the desired segmentation result. The boundary of the most likely volume of the last shrinking step serves as initial 0-level set for the 3-D level set segmentation (Fig. 8, right column). The level set method is a flexible contour and surface propagation model which can be used for 2-D and 3-D segmentation. Although it is computationally expensive, it offers several advantages for the following step. Particularly, we use its propagation flexibility when topological changes have to be managed during renal parenchyma segmentation. Level set techniques for image segmentation can be divided into contour-based [23]–[26] and region- based techniques [27]. Since the kidney shape does not vary much among several subjects, medical experts recognize kidneys in 3-Dmedical datasets with the help of prior shape information. Consequently, we will use level set models that incorporate prior shape information. Several approaches exist for prior shape level set segmentation [20], [28]–[31] also considering MR images [32], [33]. However, these approaches are mainly designed for 2-D segmentation. The authors in [32] test their method among many 2-D applications also for a 3-D dataset, but use their parametric shape model according to [28]. We regard the kernel density estimation- based shape representation used in [20] and [31] in combination with the proposed energy minimization strategy as more appropriate for a 3-D extension to our datasets. We selected and extended the work of Cremers et al. [20] for including a 3-D kidney shape representation into the level set segmentation. The authors in [20] design an energy functional consisting of a shape and an image-related part, where is a weighting parameter to guide the influence of prior shape representations

$$E(\emptyset) = \frac{1}{\propto}.E_{image}(\emptyset) + E_{shape}(\emptyset).$$

Simulation and Results

The programming language used with MATLAB is usually referred to as MATLAB script or M-script. After becoming familiar with the basic syntax of the M-script, a number of useful utilities is available that allows making extended uses of MATLAB. For example, programs are written that involves simulation. It is also used to create graphics, web pages, and GUI applications. Programs are developed using MATLAB, which can output the results to a number of media, including graphics files, HTML pages, PDF files, and Word documents. It is also possible to connect up MATLAB with other applications, such as Excel or LabView to make extended uses of it. Since it is programmed in part using Java, modification to it in the background is done using Java. The feasibility of the project is analyzed in this phase and business proposal is

put forth with a very general plan for the project and some cost estimates. The feasibility study of the proposed system is to be carried out during system analysis. This is to ensure that the proposed system is not a burden. Some understanding of the major requirements for the system is essential for feasibility analysis.

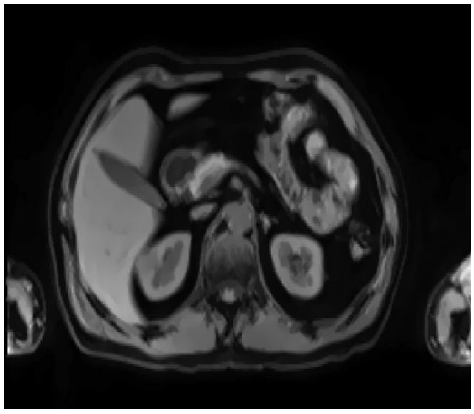

Figure 5.1: Input Kidney Image in MRI

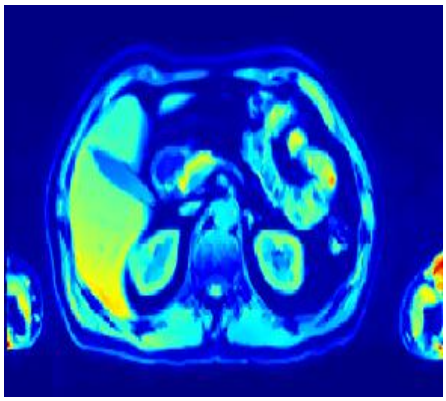

Figure 5.2: Input Images in Jet Colormap Dock (Matlab)

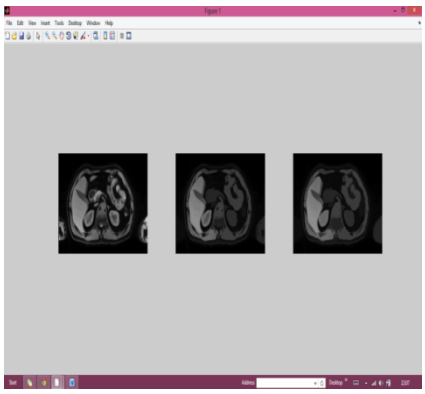

Figure 5.3: Initial Level Set Propagation

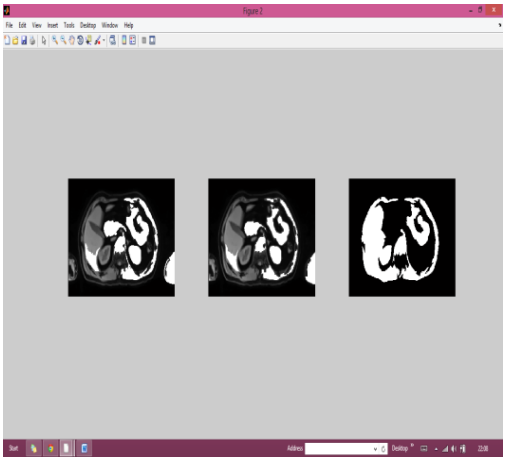

Figure 5.4: Parenchyma Cortex Edge Alignment

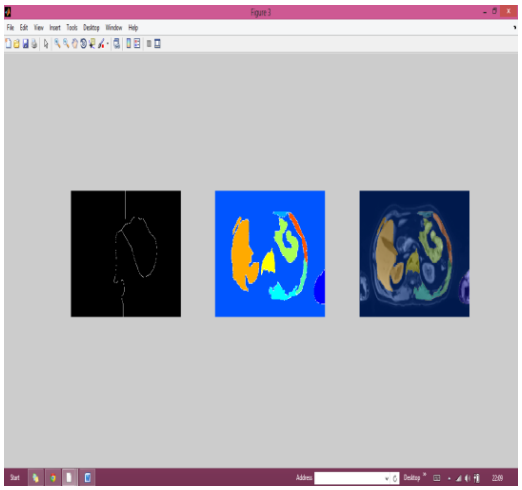

Figure 5.5: Cystic Volume Exclusion Image

Conclusion

Summary

The presented framework for fully automatic renal parenchyma volumetry is especially designed for epidemiological studies. Thus, recognized renal cystic volume will be excluded from parenchymal volume. MR Datasets showing renal cancer are excluded in SHIP. Our method is not meant to process this data as volumetry of renal cancer is usually carried out on contrast-enhanced MRI (DCE-MRI). The framework can be extended to perform kidney volumetry, if data and domain knowledge is adapted for kidney features in the training phase. However, the success for kidney segmentation and kidney volumetry needs to be tested before the adapted framework is used in clinical applications. Although 3-D parenchyma volumetry in native MR Datasets without any contrast agent is a challenging task, we presented concepts and

methods for volumetry. Since the SHIP study will give rise to other organ volumetry requests we will extend this strategy of combining trained parameters and shape models with a data-driven segmentation to other anatomical structures as well.

Future Work

However, Successful segmentation is based on an estimate of the kidney location. Consequently, limited success is to be expected for MR Datasets of participants showing abnormal locations or numbers of kidneys (i.e., in case of surgical kidney removal or congenital abnormalities in kidney location and kidney numbers). In future work, we will investigate how our shape and appearance model can be used to detect such deviation from the norm so that these cases can be handled differently.

References

[1]. Nikou, C. Bueno, S.G. Heitz, F. Armspach, J-P, "A joint physics-based statistical deformable model for multimodal brain image analysis," *Medical Imaging, IEEE Transactions on*, vol.20, no.10, pp.1026, 1037, Oct. 2001.

[2]. Marcel Prastawa, Elizabeth Bullitt, Sean Ho, Guido Gerig, "*A brain tumor segmentation framework based on outlier detection*," Elsevier Medical Image Analysis 8 (2004) 275–283.

[3]. Khalifa, F.; Beache, G.M.; Gimel'farb, G.; Giridharan, G.A.; El-Baz, A., "Accurate Automatic Analysis of Cardiac Cine Images," *Biomedical Engineering, IEEE Transactions on* , vol.59, no.2, pp.445,455, Feb. 2012.

[4]. M. Rao, J. Stough, Y.-Y. Chi, K.Muller, G. Tracton, S.M. Pizer, and EL. Chaney, "Comparison of human and automatic segmentations of kidneys from CT images," Int. J. Radiat. Oncol. Phys., vol. 61, no. 3, pp. 954–960, 2005.

[5]. B. Tsagaan, A. Shimizu, H. Kobatake, K. Miyakawa, and Y. Hanzawa, Segmentation of Kidney by Using a Deformable Model. Thessaloniki, Greece: , 2001, pp. 1059–1062.

[6]. M. Spiegel, D.-A. Hahn, V. Daum, J. Wasza, and J. Hornegger, "Segmentation of kidneys using a new active shape model generation technique based on non-rigid image registration,"Comput. Med. Imag. Graphics, vol. 33, no. 1, pp. 29–39, 2009.

[7]. Z. Lao, D. Shen, A. Jawad, B. Karacali, D. Liu, E. Melhem, R. Bryan, and C. Davatzikos, "Automated segmentation of white matter lesions in 3D brain MRI, using multivariate pattern classification," in Proc. IEEE Int. Symp. Biomed. Imaging (ISBI), 2006, pp. 307–310.

[8]. P. Anbeek, K. L. Vincken,M. J. van Osch, R. H. Bisschops, and J. van der Grond, "Automatic segmentation of different-sized white matter lesions by voxel probability estimation," Med. Image Anal., vol. 8, no. 3, pp. 205–215, 2004.

[9]. P. Anbeek, K. Vincken, M. van Osch, R. Bisschops, and J. van der Grond, "Probabilistic segmentation ofwhite matter lesions inMRimaging," NeuroImage, vol. 21, no. 3, pp. 1037–44, 2004.

[10]. R. de Boer, F. van der Lijn, H. A. Vrooman,M.W. Vernooij, M. A. Ikram, M. M. Breteler, andW. J. Niessen, "Automatic segmentation of brain tissue andwhite matter lesions in MRI," in Proc. IEEE Int. Symp. Biomed. Imag., 2007, pp. 652–655.

[11]. R. de Boer, H. A. Vrooman, F. van der Lijn,M.W. Vernooij, M. A. Ikram, A. van der Lugt, M. M. Breteler, and W. J. Niessen, "White matter lesion extension to automatic brain tissue segmentation on MRI," Neuroimage,vol. 45, no. 4, pp. 1151–1161, 2009.

[12]. R. Khayatia, M. Vafadusta, F. Towhidkhaha, and S.M. Nabavib, "Fully automatic segmentation of multiple sclerosis lesions in brain mr flair images using adaptivemixturesmethod andMarkov random field model," Comput. Biol. Med., vol. 38, no. 3, pp. 379–390, 2008.

[13]. R. Khayatia, M. Vafadusta, F. Towhidkhaha, and S. M. Nabavib, "A novel method for automatic determination of different stages of multiple sclerosis lesions in brain mr flair images," Comput. Med. Imag. Graph., vol. 32,no. 2, pp. 124–133, 2008.

[14]. F.Barkhof and R. Smithuis. (2007). "Multiple sclerosis," Radiology Assistant, [Online]. Available: http://www.radiologyassistant.nl/en

[15]. C. R. Jack, P. C. O'Brien, D. W. Rettman, M. M. Shiung, Y. C. Xu, R. Muthupillai, A. Manduca, R.Avula, andB. J. Erickson, "Flair histogram segmentation for measurement of leukoaraiosis volume," J. Mag. Res. Img., vol. 14, no. 6, pp. 668–676, 2001.

[16]. K. V. Leemput, F. Maes, D. Vandermeulen, and P. Suetens, "A unifying framework for partial volume segmentation of brain MR images," IEEE Trans. Med. Imag., vol. 22, no. 1, pp. 105–119, Jan. 2003.

[17]. M. A. Gonz´alez Ballester, A. P. Zisserman, and M. Brady, "Estimation of the partial volume effect in MRI," Med. Image Anal., vol. 6, no. 4, pp. 389–405, 2002.

[18]. A. Khademi, D. Hosseinzadeh, A. Venetsanopoulos, and A. R. Moody, "Nonparametric statistical tests for exploration of correlation and nonstationarity in images," in Proc. Int. Conf. Digital Signal Process., 2009, pp. 1–6.

[19]. B. Vijayakumar, Ashish Chaturvedi and K. Muthu Kumar, Brain Tumor in Three Dimenesional Magnetic Resonance Images and Concavity Analysis, International Journal of Computer Application, Issue 3, Volume 1 (February 2013),

[20]. P. Meer and B. Georgescu, "Edge detection with embedded confidence," IEEE Trans. Pattern Anal. Mach. Intell., vol. 23, no. 12, pp. 1351–1365, Dec. 2001.

[21]. A. Khademi, A. Venetsanopoulos, and A. Moody, "Edge-based PVA estimation in FLAIR MRI with WML," in Proc. IEEE Eng. Med. Biol. Soc. Conf., 2010, pp. 6114–6117.

[22]. P. H. Kvam and B. Vidakovic, Nonparametric Statistics with Applications to Science and Engineering. New York: Wiley-Interscience, 2007.

[23]. A. Popovic, M. de la Fuente, M. Engelhardt, and K. Radermacher, "Statistical validation metric for accuracy assessment in medical image segmentation," Int. J. Comput. Assist. Radiol. Surg., vol. 2, pp. 169–181, 2007.

[24]. B. Vijayakumar, Ashish Chaturvedi and K. Muthu Kumar, Effective Classification of Anaplastic Neoplasm in Huddling Stain Image by Fuzzy Clustering Method, International Journal of Scientific Research, Issue 3 volume 2, March-April 2013.

[25]. Vijayakumar, B., and Ashish Chaturvedi. "Automatic Brain Tumors Segmentation of MR Images using Fluid Vector Flow and Support Vector Machine." Research Journal of Information Technology 4.

[26]. Vijayakumar, B., and Ashish Chaturvedi. "Tumor Cut-Segmentation and Classification of MR Images using Texture Features and Feed Forward Neural Networks." European Journal of Scientific Research 85.3 (2012): 363-372.

[27]. Vijaya kumar, B., and Ashish Chaturvedi, "Idiosyncrasy Dissection and Assorting of Brain MR Images Instigating Kernel Corroborated Support Vector Machine," Archive Des Science.

[28]. Vijaya kumar, B., and Ashish Chaturvedi,"Abnormality segmentation and classification of brain MR images using Kernel based Support vector machine," Archive Des Science, Volume 66,Issue 4.